



# Tunable electromagnetically induced transparency in integrated silicon photonics circuit

ANG LI<sup>1,2,\*</sup> AND WIM BOGAERTS<sup>1,2</sup>

<sup>1</sup>Photonics Research Group, Ghent University-IMEC, Department of Information Technology, 9052 Gent, Belgium

<sup>2</sup>Center for Nano and Biophotonics (NB-Photonics), Ghent University, 9052 Gent, Belgium

\*ang.li@ugent.be

**Abstract:** We comprehensively simulate and experimentally demonstrate a novel approach to generate tunable electromagnetically induced transparency (EIT) in a fully integrated silicon photonics circuit. It can also generate tunable fast and slow light. The circuit is a single ring resonator with two integrated tunable reflectors inside, which form an embedded Fabry-Perot (FP) cavity inside the ring cavity. The mode of the FP cavity can be controlled by tuning the reflections using integrated thermo-optic tuners. Under correct tuning conditions, the interaction of the FP mode and the ring resonance mode will generate a Fano resonance and an EIT response. The extinction ratio and bandwidth of the EIT can be tuned by controlling the reflectors. Measured group delay proves that both fast light and slow light can be generated under different tuning conditions. A maximum group delay of 1100 ps is observed because of EIT. Pulse advance around 1200 ps is also demonstrated.

© 2017 Optical Society of America under the terms of the [OSA Open Access Publishing Agreement](#)

**OCIS codes:** (230.3120) Integrated optics devices; (230.5750) Resonators; (230.7408) Wavelength filtering devices; (230.7020) Traveling-wave devices; (260.2110) Electromagnetic optics.

## References and links

1. M. Fleischhauer, A. Imamoglu, and J. P. Marangos, "Electromagnetically induced transparency: Optics in coherent media," *Rev. Mod. Phys.* **77**, 633 (2005).
2. K. Totsuka, N. Kobayashi, and M. Tomita, "Slow light in coupled-resonator-induced transparency," *Phys. Rev. Lett.* **98**, 213904 (2007).
3. C. Peng, Z. Li, and A. Xu, "Optical gyroscope based on a coupled resonator with the all-optical analogous property of electromagnetically induced transparency," *Opt. Express* **15**, 3864–3875 (2007).
4. J. B. Khurgin, "Optical buffers based on slow light in electromagnetically induced transparent media and coupled resonator structures: comparative analysis," *J. Opt. Soc. Am. B* **22**, 1062–1074 (2005).
5. C. Roos, D. Leibfried, A. Mundt, F. Schmidt-Kaler, J. Eschner, and R. Blatt, "Experimental demonstration of ground state laser cooling with electromagnetically induced transparency," *Phys. Rev. Lett.* **85**, 5547 (2000).
6. M. Lukin and A. Imamoglu, "Controlling photons using electromagnetically induced transparency," *Nature* **413**, 273 (2001).
7. M. D. Lukin, M. Fleischhauer, M. O. Scully, and V. L. Velichansky, "Intracavity electromagnetically induced transparency," *Opt. Lett.* **23**, 295–297 (1998).
8. T. Oishi and M. Tomita, "Inverted coupled-resonator-induced transparency," *Phys. Rev. A* **88**, 013813 (2013).
9. H. Jing, Ş. K. Özdemir, Z. Geng, J. Zhang, X.-Y. Lü, B. Peng, L. Yang, and F. Nori, "Optomechanically-induced transparency in parity-time-symmetric microresonators," *Sci. Rep.* **5**, 9663 (2015).
10. H. Lü, Y. Jiang, Y.-Z. Wang, and H. Jing, "Optomechanically induced transparency in a spinning resonator," *Photonics Res.* **5**, 367–371 (2017).
11. D. D. Smith, H. Chang, K. A. Fuller, A. Rosenberger, and R. W. Boyd, "Coupled-resonator-induced transparency," *Phys. Rev. A* **69**, 063804 (2004).
12. Q. Xu, S. Sandhu, M. L. Povinelli, J. Shakya, S. Fan, and M. Lipson, "Experimental realization of an on-chip all-optical analogue to electromagnetically induced transparency," *Phys. Rev. Lett.* **96**, 123901 (2006).
13. L. Zhang, M. Song, T. Wu, L. Zou, R. G. Beausoleil, and A. E. Willner, "Embedded ring resonators for microphotonic applications," *Opt. Lett.* **33**, 1978–1980 (2008).
14. X. Yang, M. Yu, D.-L. Kwong, and C. W. Wong, "All-optical analog to electromagnetically induced transparency in multiple coupled photonic crystal cavities," *Phys. Rev. Lett.* **102**, 173902 (2009).

15. Y. Zhang, S. Darmawan, L. Tobing, T. Mei, and D. Zhang, "Coupled resonator-induced transparency in ring-bus-ring mach-zehnder interferometer," *J. Opt. Soc. Am. B* **28**, 28–36 (2011).
16. X. Yang, M. Yu, D.-L. Kwong, and C. W. Wong, "Coupled resonances in multiple silicon photonic crystal cavities in all-optical solid-state analogy to electromagnetically induced transparency," *IEEE J. Sel. Top. Quantum Electron.* **16**, 288–294 (2010).
17. Q. Huang, Z. Shu, G. Song, J. Chen, J. Xia, and J. Yu, "Electromagnetically induced transparency-like effect in a two-bus waveguides coupled microdisk resonator," *Opt. Express* **22**, 3219–3227 (2014).
18. Z. Zhang, G. I. Ng, T. Hu, H. Qiu, X. Guo, M. S. Rouified, C. Liu, and H. Wang, "Electromagnetically induced transparency-like effect in microring-bragg gratings based coupling resonant system," *Opt. Express* **24**, 25665–25675 (2016).
19. A. Li and W. Bogaerts, "An actively controlled silicon ring resonator with a fully tunable fano resonance," *APL Photonics* **2**, 096101 (2017).
20. A. Li and W. Bogaerts, "Fundamental suppression of backscattering in silicon microrings," *Opt. Express* **25**, 2092–2099 (2017).
21. M. Fiers, T. Van Vaerenbergh, K. Caluwaerts, D. V. Ginste, B. Schrauwen, J. Dambre, and P. Bienstman, "Time-domain and frequency-domain modeling of nonlinear optical components at the circuit-level using a node-based approach," *J. Opt. Soc. Am. B* **29**, 896–900 (2012).
22. A. Li, Q. Huang, and W. Bogaerts, "Design of a single all-silicon ring resonator with a 150 nm free spectral range and a 100 nm tuning range around 1550 nm," *Photonics Res.* **4**, 84–92 (2016).
23. A. Li, T. Vaerenbergh, P. Heyn, P. Bienstman, and W. Bogaerts, "Backscattering in silicon microring resonators: a quantitative analysis," *Laser Photonics Rev.* **10**, 420–431 (2016).
24. B. Peng, S. K. Ozdemir, W. Chen, F. Nori, and L. Yang, "What is-and what is not-electromagnetically-induced-transparency in whispering-gallery-microcavities," *arXiv preprint arXiv:1404.5941* (2014).
25. P. Dumon, W. Bogaerts, R. Baets, J.-M. Fedeli, and L. Fulbert, "Towards foundry approach for silicon photonics: silicon photonics platform epixfab," *Electron. Lett.* **45**, 581–582 (2009).
26. W. Bogaerts, P. De Heyn, T. Van Vaerenbergh, K. De Vos, S. Kumar Selvaraja, T. Claes, P. Dumon, P. Bienstman, D. Van Thourhout, and R. Baets, "Silicon microring resonators," *Laser Photonics Rev.* **6**, 47–73 (2012).
27. Q. Li, Z. Zhang, J. Wang, M. Qiu, and Y. Su, "Fast light in silicon ring resonator with resonance-splitting," *Opt. Express* **17**, 933–940 (2009).

## 1. Introduction

*Electromagnetically induced transparency* (EIT) is a fundamental phenomenon originally shown in atomic physics [1]. Due to the destructive interference of the transition probability amplitude between atomic states, EIT will generate an ultra narrow "transparent window" in the transmission or absorption spectrum as shown in Fig. 1. The amplitude response is accompanied by extreme dispersion due to an abrupt phase change within this ultra narrow window, which translates to a very large group index  $n_g$  or slow group velocity  $v_g$ .

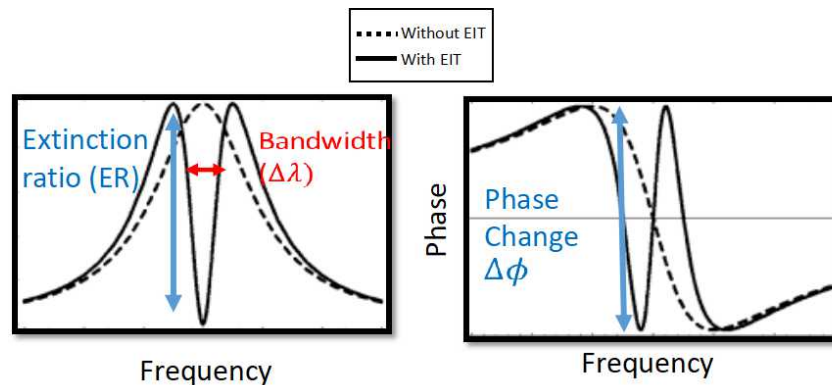


Fig. 1. The spectral characteristics of EIT based on Fig. 1 from [1]. It will generate an ultra narrow window in the transmission or absorption spectrum. And the phase response or index profile shows an abrupt change within this window.

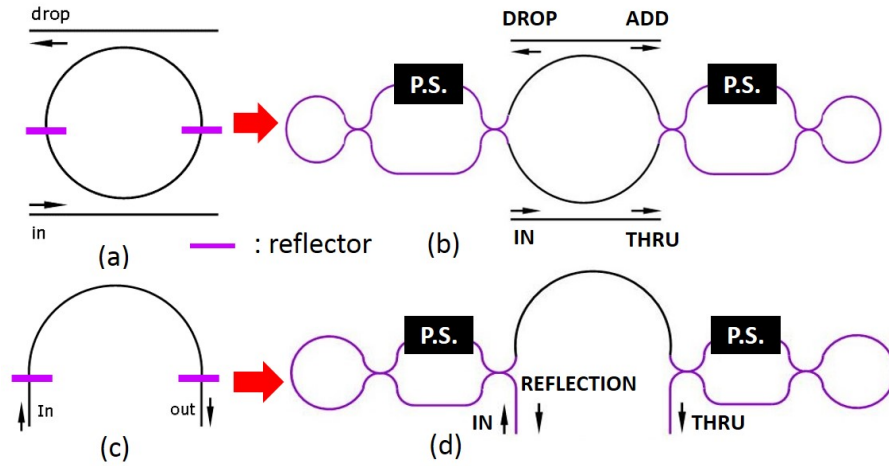


Fig. 2. Conceptual schematics of the complete device and the embedded FP cavity formed by two reflectors are given in (a) and (c), while (b) and (d) show the concrete schematics of them where the loop-ended MZI reflectors are included. *P.S.* stands for phase shifter.

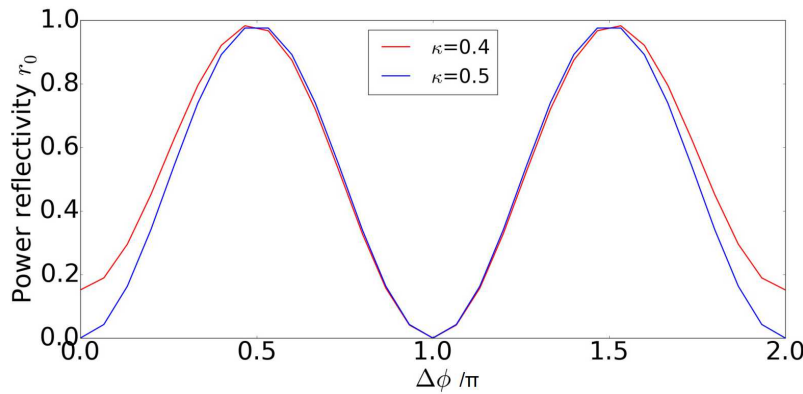


Fig. 3. Simulated tunability of the reflector. Note the difference of the power reflectivity at the beginning state ( $\Delta\phi = 0$ ) for perfect 50/50 directional couplers (power coupling coefficient  $\kappa = 0.5$ ) and imperfect directional couplers.

In past decades, the optical analogue of EIT has attracted strong attention and has been intensively researched, as this extreme dispersion in optical signal will be very promising to demonstrate slow light or even stopped light, for applications in optical gyroscopes, optical buffers, laser cooling, optical switching and other nonlinear optics [2–6]. Many efforts have been taken to demonstrate EIT in various platforms [7–10]. However, for those applications, it's either highly desirable or necessary to be implemented in a *photonic integrated circuit* (PIC). Silicon photonics has grown to be one of the most promising and attractive platforms for PICs due to its ultra-high index contrast and CMOS compatibility, which allow compact components and high-volume, low-cost fabrication. Various approaches to demonstrate the optical analogue to EIT in silicon photonics have been reported over the past years [11–18]. Most demonstrations rely on coupled cavities to generate EIT due to their similarity with atomic systems [11–16]. However, fabrication variations between those cavities, whether they are ring resonator or photonic crystal based, form an inevitable performance limiting issue. Moreover, all demonstrations lack a mechanism for

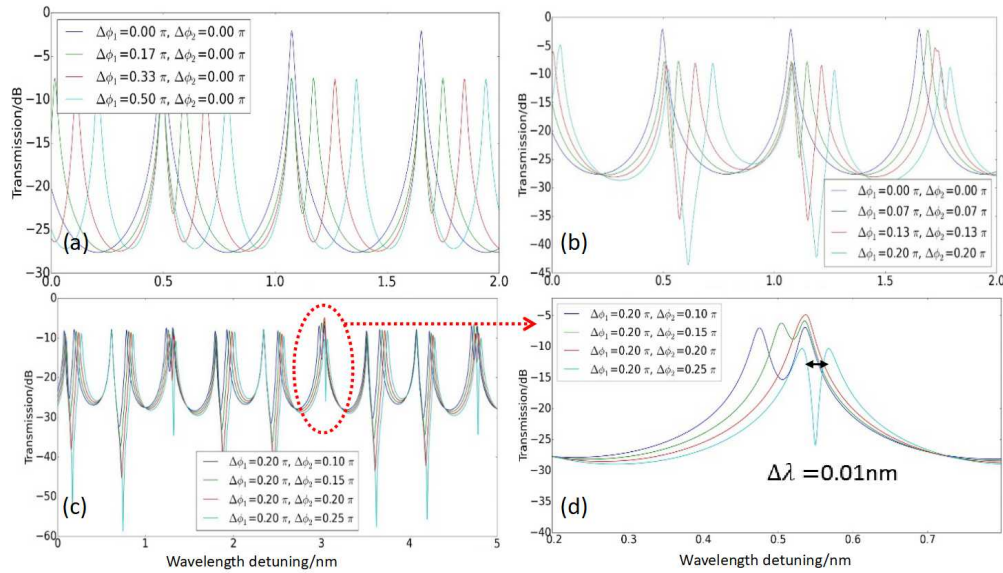


Fig. 4. Simulated output at the drop port of the device. Without any reflections, we see a Lorentzian-shaped resonance. Increasing one reflector's reflectivity leads to normal resonance splitting (a); When the second reflector also introduces reflection, a Fano resonance appears from the interference between a FP mode and a ring resonance (b); An EIT like spectrum can be generated by precisely adjusting the reflectors' reflectivities (c). A zoom view of one resonance (d).

efficient tuning of the key properties of the EIT spectra and the physical factors that influence them. For instance, the distance between cavities determines the inter-cavity coupling strength, but can only be physically adjusted. What's more, the use of multiple cavities imposes extra complexity and footprint. Some other approaches utilizing sidewall gratings on the bus waveguide of a single resonator have also been reported [17, 18], but these suffer from the same problem of poor tunability of the physical parameters. What's more, the requirement of E-beam lithography to define those high definition sidewall gratings weakens the advantage of silicon photonics.

In this paper, we propose and experimentally demonstrate a novel approach towards EIT using a silicon photonic integrated circuits. The circuit is a single silicon ring resonator with two integrated tunable reflectors inside, which form an embedded Fabry-Perot (FP) cavity inside the ring cavity, whose output mode depends on the reflectivity of the reflectors. By controlling the reflectivity through thermo-optic phase shifters (metal heaters), the interference of the FP mode and ring resonance mode can be tuned to exhibit different patterns including a single ring resonance mode, normal resonance splitting, Fano resonances and an EIT-like spectrum [19]. The spectral features of the EIT including extinction ratio and phase change can also be tuned.

## 2. Device design and simulation

As mentioned above, our device is a single ring resonator with two integrated tunable reflectors inside. The EIT comes from the interference of the high Q ring resonance mode and the low Q FP mode formed by those reflectors. In Fig. 2, both the conceptual and concrete schematics of the complete device and the FP cavity formed by the reflectors are given. The curves drawn in violet indicate the two tunable reflectors, which are loop-ended symmetric *Mach-Zehnder interferometers* (MZI). Its reflectivity can be efficiently tuned from 0 to almost 100% by adding

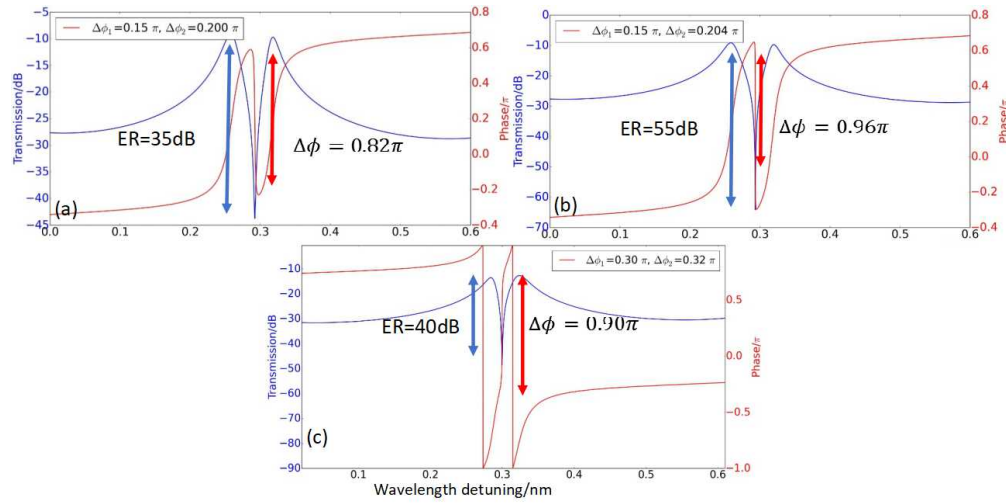


Fig. 5. Tunability and phase response of the ring with two reflectors. By tuning the relative phase shift of the reflectors, we can get various EIT resonances. The extinction ratio can be over 55 dB and the phase change can be as large as  $0.96\pi$  within 0.01 nm bandwidth. This can be translated to a group index around 300 and a Q factor of this EIT peak around  $1.54 \times 10^5$ .

$0.5\pi$  radians to the phase shifter, which can be a metal heater on top of one arm of the MZI or a doped silicon waveguide heater sitting next to it [20]. This wide tuning range of the reflectivity makes it possible to get diverse FP modes that serve as background modes to interfere with the high Q ring resonance mode.

We use a commercial optical circuit simulator-Caphe to simulate our device [21]. The directional couplers of the reflectors are designed to be 50/50 splitter for simple demonstration. This condition guarantees that at beginning (without extra phase shift) the reflectors have zero reflectivity as shown in Fig. 3. In reality, fabrication variation shifts the directional couplers slightly off the ideal 50/50 ratio, which means that without any phase shift the reflectors already introduce certain reflections [22]. However, as shown in Fig. 3, it is always possible to obtain a reflectivity range of 0-100%, even with imperfect reflectors.

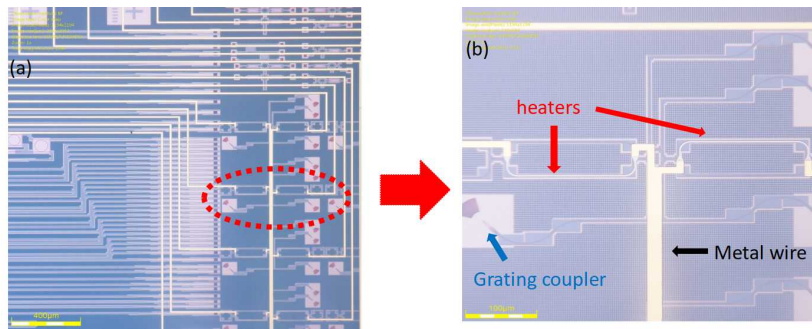


Fig. 6. Microscopic images of our devices(a) and a zoom view of a single device (b).

In Fig. 4 we plot the simulated spectra of the device under different phase shifts of the reflectors. At original state, the reflectivity is zero, so it's a pure ring resonator with Lorentzian-shape resonance at the drop port of the device as shown in Fig. 4(a). Then we add phase shift to one of



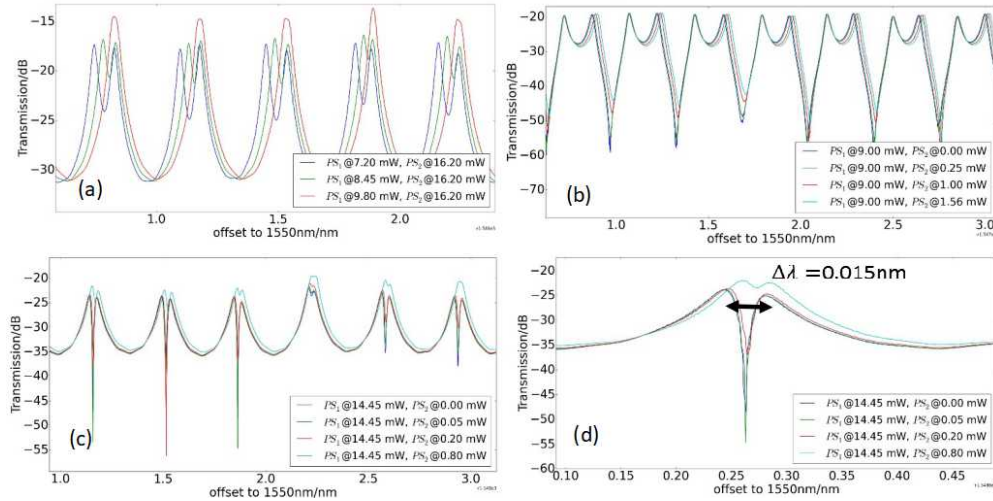


Fig. 7. Measured transmission spectra corresponding with the simulated spectra shown in Fig. 4. (a) presents the cases of Lorentzian-shaped resonance and normal resonance splitting where only one reflector introduces reflection. (b) indicates the Fano resonances when both reflectors introduce reflections. (c) gives the spectrum with EIT resonance. (d) provides a zoom view of one resonance in (c). It shows a bandwidth around 0.015 nm, or a Q factor around  $1 \times 10^5$ . All the measured spectra match well with simulations.

the two reflectors to increase its reflectivity while keeping the other at zero reflection. Figure 4(a) shows the appearance of resonance splitting starts due to the internal reflection that couples the clockwise and counter-clockwise propagation modes and break their degeneracy [23]. Figure 4(b) shows the results If we then increase the second reflector's reflectivity, a sharp Fano resonance starts to appear as now the output at drop port is an interference between the FP cavity mode and the ring resonance mode. Precisely adjusting the reflectors can generate EIT-like spectrum as shown in Fig. 4(c). The transition from Fano resonance to EIT is in consistent with former literature [24], and the simulated phase responses shown in Fig. 5 also serve as proof of EIT [1], exhibiting the very abrupt phase change. The differences between adjacent resonance groups in the spectrum originate in the dispersive behavior of the waveguides and directional couplers included in our model, which will influence the alignment between the FP mode and the ring resonances.

The EIT features including extinction ratio, bandwidth and phase change can be further tuned by controlling the reflectors, as shown in Fig. 5. The phase change can be as large as  $0.96\pi$  within 0.01 nm optical bandwidth which indicates a very strong dispersion within this narrow window with a group index  $n_g = 300$  and a Q factor of this EIT peak as large as  $Q_{eit} = 1.54 \times 10^5$ .

### 3. Experimental results

Figure 6 gives the microscopic images of the fabricated devices. The devices are fabricated on a 220 nm SOI wafer through MPW service at IMEC's 200mm CMOS technology line [25]. Structures are covered by top silicon dioxide with a thickness of  $1.5 \mu\text{m}$ . The metal heaters are post-processed using Titanium as resistive element and Gold as conducting wires. The heater has a width of  $2 \mu\text{m}$  and a thickness of 100 nm. We choose its length to be  $200 \mu\text{m}$  to guarantee adequate phase shift but the experimental results show that it can be safely reduced to  $100 \mu\text{m}$  or even shorter with more efficient heaters, for instance, side doped silicon waveguides.

The measured amplitude spectra are plotted in Fig. 7. Similar to simulation results shown in

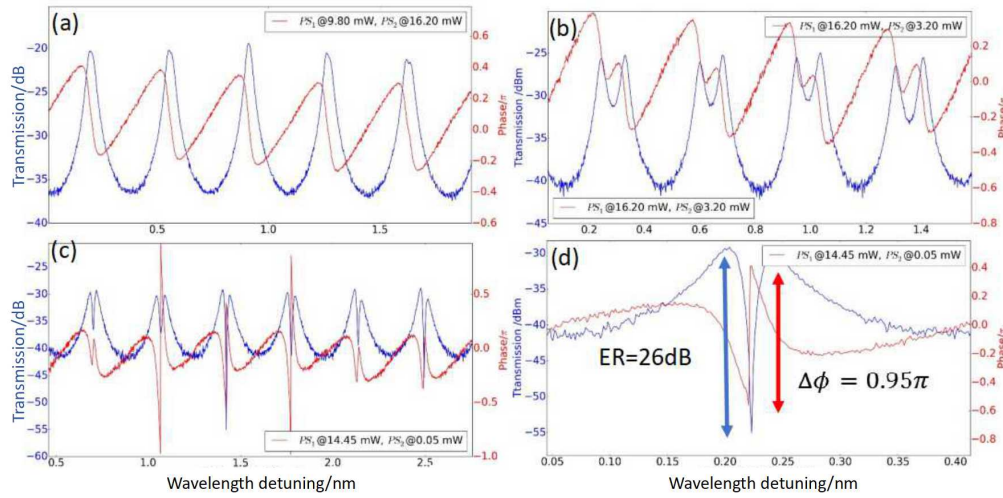


Fig. 8. Measured phase response for the Lorentzian-shaped resonance (a), normal resonance splitting (b) and EIT resonance (c). When EIT is present, an abrupt phase change happens within its ultra narrow bandwidth. The largest phase change can be  $0.95\pi$  within 0.015 nm span. This means a group index of 200 and a Q factor of  $1 \times 10^5$ .

Fig. 4, we also plot 3 measured spectra of different patterns to present the good matching between simulations and measurements. In Fig. 7(a), we plot the spectra of Lorentzian-shaped resonances where both reflectors introduce zero or very low reflections as well as the normal resonance splitting case where only one reflector introduces strong reflection. If we further increase the second reflector's reflectivity, the Fano resonance starts to appear, as shown in Fig. 7(b). The spectra with EIT-feature is given in Fig. 7(c) and a zoom view of one EIT resonance is plotted in Fig. 7(d). All these measurements show a good one-to-one matching with those simulated spectra.

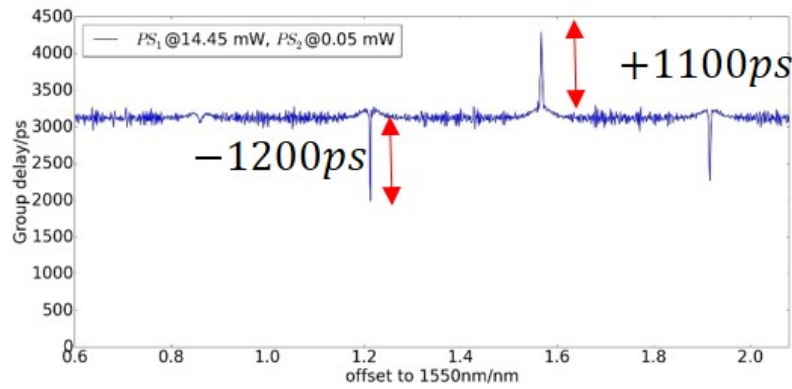


Fig. 9. Measured group delay of the spectrum shown in Fig. 8(c). At the EIT peak, there is a larger group delay at 4100 ps, compared to the background level at 3200 ps, the EIT slows light down at 1100 ps. We also notice some dips at the delay spectrum at the resonances showing splitting. This is the so-called fast light phenomenon. Due to our tunability of the internal reflections, we can achieve both tunable fast light and slow light.

To get the phase response, we use an optical vector network analyzer (OVNA) from Luna Inc. to perform the measurements. It has an integrated interferometer that helps to extract the phase

responses from our chip. The wavelength resolution is 1.5 pm. The results are given in Fig. 8. We list three sets of phase measurements, corresponding with the pure Lorentzian-shaped resonance pattern, normal resonance splitting pattern and EIT resonance pattern. Consistent with former literature, when it's pure ring resonance, the abrupt phase change only happens near the resonance wavelength [26]. While at the resonance splitting case, there is a gradual phase change in the splitting region. This phenomenon can be used to demonstrate fast light [27]. While at the EIT resonance, there is an abrupt phase change as large as  $0.95\pi$  within its 0.015 nm bandwidth. The calculated group index  $n_g$  is around 200. We also give the measured group delay of such a device using the same equipment. Results of the spectrum shown in Fig. 8(c) are given in Fig. 9. Clearly, at the EIT peak, the group delay is 1100 -ps larger than the background level. What's more, for the other peak where it shows resonance splitting, we observe a smaller group delay, indicating a pulse advance. This is the so-called fast light effect introduced by resonance splitting [27]. Due our ability to fully control of the reflections inside the ring cavity (thus the resonance splitting conditions), we are able to get a larger pulse advancement ( 1200 ps in our case) than former literature [27]. The tunability of the EIT resonance can also be viewed in Fig. 8(c).

#### 4. Conclusion

In this paper, we propose a novel method towards tunable EIT in a fully integrated silicon photonics circuits consisting of a silicon ring resonator with two integrated tunable reflectors. The FP cavity formed by those reflectors can interfere with the ring resonance to generate various patterns, including Fano resonances and EIT resonances. We perform rigorous simulations of the transmission spectra, phase responses and tunability. Experimental characterizations are also provided. The measured transmission spectra and phase responses show a good matching with simulated results. The device can be simply and efficiently tuned with top metal heaters or more efficient phase shifters. An EIT resonance with an extinction ratio over 25 dB, a Q factor around  $1 \times 10^5$  and a phase jump of  $0.95 \pi$  within 0.015 nm optical span is observed. This device offers a new and effective approach to on-chip EIT based applications.